PIECEWISE-LINEAR EXPANSIONS FOR NONLINEAR ACTIVE NOISE CONTROL

Giovanni L. Sicuranza

DEEI - University of Trieste
Via A. Valerio, 10 - 34127 Trieste, Italy
email: sicuranza@univ.trieste.it

Alberto Carini

STI - University of Urbino
Piazza della Repubblica, 13 - 61029 Urbino, Italy
email: carini@sti.uniurb.it

ABSTRACT

Functional link artificial neural networks exploiting orthogonal functional expansions have been recently proposed as efficient structures for nonlinear active noise control. In this paper it will be shown that simple piecewise-linear expansions can effectively replace trigonometric and orthogonal polynomial expansions. The controller is adapted using an extension of the Affine Projection algorithm we recently proposed and studied with reference to its transient and steady-state behavior.

1. INTRODUCTION

While the majority of ANC systems applied in practice are linear, in the last years the relevance of the nonlinear effects in actual applications has been widely recognized. Different nonlinear filtering structures have been proposed in the literature to cope with nonlinearities. Among them, Volterra filters have been widely adopted [1], [2], [3]. More recently, functional link artificial neural networks (FLANN) were proposed in [4] as an alternative to Volterra filters. Like in the case of Volterra filters, the output of a FLANN structure depends linearly from the filter coefficients. However, in contrast to the Volterra filters, where the terms multiplied by the coefficients are products of present and past input samples, FLANNs employ nonlinear functional expansions of the present sample. Moreover, it is worth noting that both Volterra and FLANN filters can be efficiently implemented in the form of filter banks, as shown in [2], [3], [4].

It was also shown in [4] that FLANNs using trigonometric functional expansions and a variation of the Filtered-X LMS algorithm can provide in some cases better behaviors than Volterra filters adapted with an equivalent algorithm.

In this paper we will consider FLANN structures exploiting very simple piecewise linear (PWL) functional expansions. We will show that even better performances than with more complex orthogonal expansions can be obtained. Moreover, we extend to the these structures the Affine Projection (AP) adaptation algorithms previously applied to Volterra filters [3]. The transient and steady-state behaviors of these algorithms have been studied in [5]. Since the filters equipped with PWL functional expansions belong to the class of filters whose output depend linearly from the filter coefficients, it is possible to extend to them this analysis and thus to motivate the good performances obtained.

The paper is organized as follows. In Section 2 the exact and an approximate adaptation algorithms studied in [5] are reformulated to be applied to the structures based on functional expansions in the general case of a multichannel ANC scheme. In Section 3 the nonlinear active noise controller based on PWL functional expansions is described in detail. Simulation results are presented and discussed in Section 4 with reference to a narrow-band noise source in a single channel environment and to a wide-band noise source in a multichannel environment. Concluding remarks are presented in Section 5.

This work was supported by the MIUR under Grant PRIN 2004092314.

2. FILTERED-X AFFINE PROJECTION ALGORITHMS

The simplified scheme of a multichannel feed-forward active noise controller with I noise source signals, J actuators signals and K error sensors is shown in Figure 1.

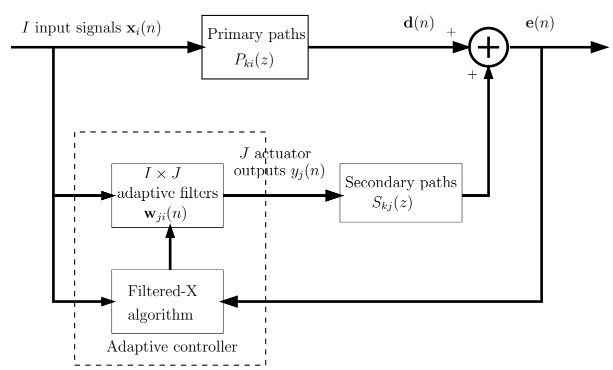

Fig. 1. Multichannel feedforward active noise controller.

It is assumed here that the models of the secondary paths are available. The j-th actuator output is modeled as

$$y_j(n) = \sum_{i=1}^{I} \tilde{\mathbf{x}}_i^T(n)\mathbf{w}_{j,i}(n), \tag{1}$$

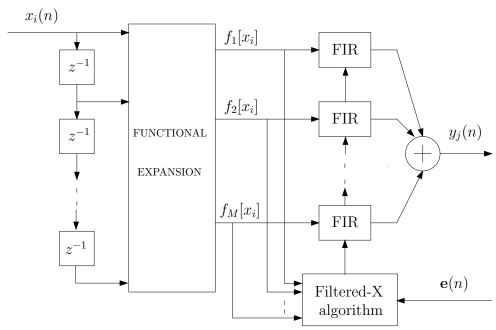

Fig. 2. Filter implementation using functional expansions.

where $\mathbf{w}_{ji}(n)$ is the coefficient vector of the filter connecting the input i to the output j of the adaptive controller, and $\tilde{\mathbf{x}}_i(n)$ is the i-th signal vector at the input of the adaptive part of the controller, which in our approach is expressed as a vector function of the noise source samples x_i. Its general form is given by

$$\tilde{\mathbf{x}}_i(n) = \left[f_1\left[x_i\right], f_2\left[x_i\right], \ldots, f_M\left[x_i\right]\right]^T, \tag{2}$$

where $f_i[\cdot]$, for any $i = 1 \ldots M$, is a time invariant functional of its argument. Equations (1) and (2) include linear filters, truncated Volterra filters of any order p [3] and other nonlinear functionals as the FLANN structures proposed in [4]. The realization of a filter belonging to such a class of filters is shown in Figure 2. In the case of Volterra filters, the functional expansions involve the present and past input samples whose products are then suitably delayed by the FIR filters. In contrast, only functional expansions of the present input sample are used in the FLANN case, as shown in Section 3.

It is worth noting that in the multichannel case every filter in the controller is implemented according to this structure.

To introduce the Filtered-X AP algorithms applied to the FLANN structures, the following notations are used:
L is the affine projection order,
N_t is the number of elements of vectors $\tilde{\mathbf{x}}_i(n)$ and $\mathbf{w}_{j,i}(n)$,
$N_t \cdot I \cdot J$ is the number of coefficients of $\mathbf{w}(n)$,
$\mathbf{x}_i(n)$ is the i-th primary source input signal vector,
$\tilde{\mathbf{x}}_i(n)$ is the functionally expanded i-th input signal vector
$\tilde{\mathbf{x}}(n) = \left[\tilde{\mathbf{x}}_1^T(n), \ldots, \tilde{\mathbf{x}}_I^T(n)\right]^T$, is the full functionally expanded input signal vector,
$\mathbf{w}_{j,i}(n)$ is the coefficient vector of the filter connecting the input i to the output j of the controller,
$\mathbf{w}_j(n) = \left[\mathbf{w}_{j,1}^T(n), \ldots, \mathbf{w}_{j,I}^T(n)\right]^T$ is the aggregate of the coefficient vectors at the output j of the controller,
$\mathbf{w}(n) = \left[\mathbf{w}_1^T(n), \ldots, \mathbf{w}_I^T(n)\right]^T$ is the full coefficient vector of the controller,
$y_j(n) = \mathbf{w}_j^T(n)\tilde{\mathbf{x}}(n)$ is the j-th secondary source signal,
$d_k(n)$ is the output of the k-th primary path,
$\mathbf{d}_k(n) = \left[d_k(n), \ldots, d_k(n-L+1)\right]^T$ is the vector of the L past outputs of the k-th primary path,
$\mathbf{d}(n) = \left[\mathbf{d}_1^T(n), \ldots, \mathbf{d}_K^T(n)\right]^T$ is the full vector of the L past outputs of the primary paths,
$s_{k,j}(n)$ is the impulse response of the secondary path connecting the j-th secondary source to the k-th error sensor,
$\mathbf{u}_{k,j}(n) = s_{k,j}(n) \odot \tilde{\mathbf{x}}(n)$ is the Filtered-X vector obtained by filtering, sample by sample, $\tilde{\mathbf{x}}(n)$ with $s_{k,j}(n)$,
$\mathbf{u}_k(n) = \left[\mathbf{u}_{k,1}^T(n), \ldots, \mathbf{u}_{k,J}^T(n)\right]^T$ is the aggregate of the Filtered-X vectors associated with the output k,
$\mathbf{U}_k(n) = \left[\mathbf{u}_k(n), \mathbf{u}_k(n-1), \ldots, \mathbf{u}_k(n-L+1)\right]$ is the matrix constituted by the last L Filtered-X vectors $\mathbf{u}_k(n)$,
$\mathbf{U}(n) = \left[\mathbf{U}_1(n), \ldots, \mathbf{U}_K(n)\right]$ is the full matrix of Filtered-X vectors,
$e_k(n) = d_k(n) + \sum_{j=1}^{J} s_{k,j}(n) \odot y_j(n)$ is the k-th error sensor signal,
$\mathbf{I}$ indicates an identity matrix of appropriate dimensions,
$\odot$ denotes the linear convolution,
diag$\{\ldots\}$ is a block-diagonal matrix of the entries $\{\ldots\}$.

The AP algorithms applied in this paper to the filters in (1) and (2) are the singlechannel or multichannel exact AP algorithm and an approximate AP algorithm introduced in [5].

The adaptation rules of the two algorithms can be put in the same form as follows

$$\mathbf{w}(n+1) = \mathbf{w}(n) - \boldsymbol{\mu}\overline{\mathbf{U}}(n)\mathbf{e}(n), \tag{3}$$

where $\boldsymbol{\mu}$ is a diagonal step-size matrix and the matrix $\overline{\mathbf{U}}(n)$ is defined according to equations (4) and (5) in case of the exact and the approximate algorithms respectively,

$$\overline{\mathbf{U}}(n) = \mathbf{U}(n)\left[\mathbf{U}^T(n)\mathbf{U}(n) + \delta\mathbf{I}\right]^{-1}, \tag{4}$$

$$\overline{\mathbf{U}}(n) = \mathbf{U}(n) \cdot \text{diag}\left\{\left[\mathbf{U}_1^T(n)\mathbf{U}_1(n) + \delta\mathbf{I}\right]^{-1}, \ldots \right.$$
$$\left. \ldots, \left[\mathbf{U}_K^T(n)\mathbf{U}_K(n) + \delta\mathbf{I}\right]^{-1}\right\}, \tag{5}$$

where δ is a small positive constant. It is worth noting that in the singlechannel case, where $I = J = K = 1$, the adaptation equations of (3) and (5) reduces to the adaptation rule of the exact AP algorithm given by (3) and (4).

3. THE ACTIVE NOISE CONTROLLER BASED ON PIECEWISE-LINEAR FUNCTIONAL EXPANSIONS

In the FLANN case the resulting structure of a filter in the controller is simplified as shown in Figure 3. Only functional expansions of the present input sample are used and then delayed by the FIR filters, as in the case of Volterra filters.

In this paper we propose to use only one PWL functional expansion since, in contrast to what stated in [4], it is not necessary to resort to orthogonal expansions for efficiently dealing with nonlinearities. Any admissible PWL function is required to be an input-output mapping with a discontinuity in the function itself or in its derivative. Among all the possible choices, the functions named ABS and SIGN in Figure 4 have been tested in order to minimize the implementation complexity. The bounds of the definition domain are

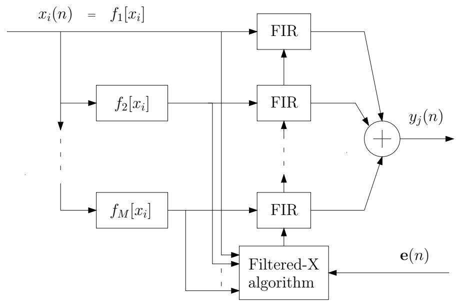

Fig. 3. Filter implementation using FLANN expansions.

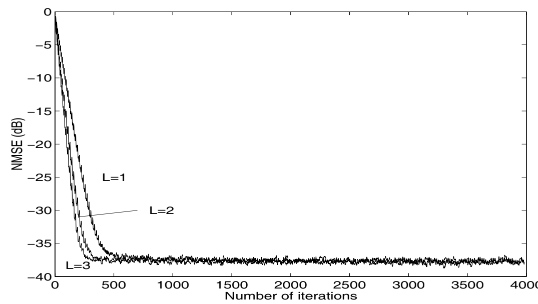

Fig. 5. Attenuation at the error microphone.

fixed as the minimum and the maximum values of the input signal, x_{min} and x_{max} respectively. The ABS PWL function can be easily computed as $f_2[x_i] = |x_i(n) - a|$, where $a = (x_{min} + x_{max})/2$. Therefore, the $N_t \times 1$ vector $\tilde{\mathbf{x}}_i(n)$ in (1) is given by

$$\tilde{\mathbf{x}}_i(n) = \big[x_i(n),\ x_i(n-1), \ldots, x_i(n-N+1),\\ |x_i(n) - a|, \ldots, |x_i(n-N+1) - a|\big]^T. \tag{6}$$

where N is the memory length of the two FIR filters and thus $N_t = 2N$. The SIGN PWL function can be expressed as $f_2[x_i] = sign\big(x_i(n) - b\big)\big(x_i(n) - a\big)$, where $b = x_{min} + (x_{max} - x_{min})/4$. It is worth noting that the preliminary knowledge of the range of the input signal is required. However, it has been noted that, in general, even a rough evaluation of the minimum and maximum values allows good performances in the adaptation procedure. The rational for using such kinds of functional expansions can be appreciated in the two main cases [1], [2] where nonlinear effects are important, i. e., when a) the primary paths include some nonlinearities and b) the noise is modelled as a chaotic signal.

In the first case, in fact, high order harmonics are generated by the primary paths that need to be re-created in the secondary paths. The above defined PWL functions are able to furnish these high order harmonics whose amplitudes and phases are adjusted by the adaptive part of the controller. A simulation result illustrating this principle for a narrow-band scheme will be described in the next section.

In the second case, even though the previous argument can be in principle still exploited, we prefer to resort to the theory presented in [5] to validate our results. The expressions for the MSD and MSE in [5] can be suitably adapted, according to this theory, to deal with the functional expansions proposed here. Due to the lack of space, these expressions can not be explicitly presented in this paper. Nevertheless, an example of the results obtained for a wide-band multichannel scheme will be commented in Section 4, so that the good performances obtained with PWL functions can be supported by theoretically derived arguments.

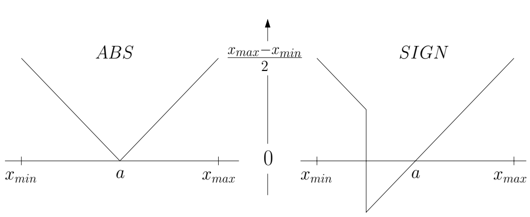

Fig. 4. PWL functional expansions.

4. SIMULATION RESULTS

A. Single-channel narrow-band experiment.

The simulation environment is that of Experiment III in [4]. The input noise is a sinusoidal signal at 500 Hz sampled at 8000 samples/s and corrupted with a Gaussian noise with 40 dB of attenuation. The primary path is characterized by a nonlinear input-output relationship

$$d_p(n) = u(n-2) + 0.08u^2(n-2) - 0.04u^3(n-1)) \tag{7}$$

applied to the input samples filtered with the FIR transfer function

$$F(z) = z^{-3} - 0.3z^{-4} + 0.2z^{-5}. \tag{8}$$

Therefore, the nonlinear combination produces high order harmonics. The secondary path is characterized by the nonminimum phase transfer function

$$S(z) = z^{-2} + 1.5z^{-3} - z^{-4}. \tag{9}$$

The structures used in the controller are the PWL functional expansions in Figure 4. The length of the FIR filters has been fixed equal to 10 so that the total number of coefficients is equal to 20. Figure 5 shows the adaptation curves obtained by using the SIGN function in addition to the linear channel. In this figure, the ensemble averages at the error microphone for 50 runs of the adaptation algorithm in (3), (5) for the affine projection order $L = 1, 2, 3$ are reported. The ensemble averages are normalized to the power of unattenuated noise at the error microphone as in [4]. The constant δ is set equal to 0.001 and the step size is chosen equal to 0.0560. The diagrams in Figure 5 show the good convergence behavior and the effect of the AP order.

e_{4000}	L=1	L=2	L=3
FLANN sin/cos	-37.2	-37.1	-37.1
ABS	-36.7	-36.9	-37.3
SIGN	-37.7	-37.8	-37.9

Table 1. NMSE at 4000 iterations.

Table 1 reports the mean residual errors at 4000 iterations for the 3-channel structure equipped with the sine and cosine functions as in [4], and the 2-channel structures equipped with the ABS and SIGN functions. The comparisons have been made by choosing for the different configurations the step sizes which guarantee close convergence speeds, measured by a residual error at the iteration $n = 250$ equal to $-25.0 \pm 0.1dB$ for $L = 1$. The results in Table 1 show that PWL expansions can offer similar or even better performances than usual FLANNs.

B. Multichannel wide-band experiment.

In this experiments we consider a multichannel active noise controller with $I = 1$, $J = K = 2$ as in the experiment C in [5]. The transfer functions of the primary and secondary paths are

$$\begin{aligned}
p_{1,1}(z) &= 1.0z^{-2} - 0.3z^{-3} + 0.2z^{-4}, \\
p_{2,1}(z) &= 1.0z^{-2} - 0.2z^{-3} + 0.1z^{-4}, \\
s_{1,1}(z) &= 2.0z^{-1} - 0.5z^{-2} + 0.1z^{-3}, \\
s_{1,2}(z) &= 2.0z^{-1} - 0.3z^{-2} - 0.1z^{-3}, \\
s_{2,1}(z) &= 1.0z^{-1} - 0.7z^{-2} - 0.2z^{-3}, \\
s_{2,2}(z) &= 1.0z^{-1} - 0.2z^{-2} + 0.2z^{-3}.
\end{aligned}$$

The input signal is the normalized logistic noise [1] and the controller employs the ABS functional expansion and two FIR filters of length 4.

Figure 6 diagrams the steady-state MSE of the exact (upper curves) and approximate (lower curves) AP Filtered-X algorithms estimated according to the theory in [5] and obtained from simulations with time averages over 10 billion samples, at different values of step-size μ and for the AP order $L = 1, 2$ and 3. In Fig. 6 the theoretical values (solid lines) of MSE fall close to the corresponding simulation values (dashed lines). The approximate algorithm in (3) and (5) provides better MSE values than the exact algorithm in (3) and (4). However, it provides also a lower convergence speed than the exact algorithm, as confirmed by Figure 7 where the evolution of the residual errors are plotted for the step-size $\mu = 0.007813$, together with the corresponding steady-state MSE values (dashed lines). Again, the upper curves refer to the exact algorithm, while the lower ones refer to the approximate algorithm. It is worth noting that these performances are better than those obtained with Volterra filters in [5].

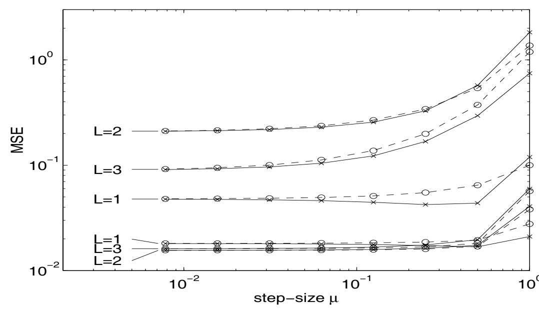

Fig. 6. MSE with the ABS function

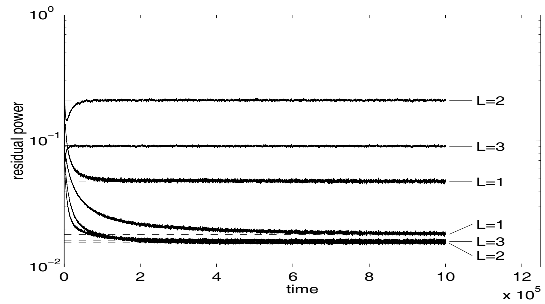

Fig. 7. Residual errors with the ABS function

5. CONCLUDING REMARKS

In this paper exact and approximate Filtered-X AP algorithms have been extended to structures using functional expansions. It has been shown that simple PWL functions can be exploited to deal with nonlinearities in ANC. The relevant result is that efficient controllers can be designed as filter banks in which the nonlinear channel has the same complexity of the linear channel.

6. REFERENCES

[1] P. Strauch and B. Mulgrew, “Active control of nonlinear noise processes in a linear duct,” *IEEE Trans. Signal Processing*, vol. 46, pp. 2404-2412, Sept. 1998.

[2] L. Tan and J. Jiang, “Adaptive Volterra filters for active noise control of nonlinear processes,” *IEEE Trans. Signal Processing*, vol. 49, pp. 1667-1676, Aug. 2001.

[3] G. L. Sicuranza and A. Carini, “A Multichannel Hierarchical Approach to Adaptive Volterra Filters employing Filtered-X Affine Projection Algorithms,” *IEEE Trans. Trans. Signal Processing*, vol. 53, No. 4, pp. 1463-1473, April 2005.

[4] D. D. Das and G. Panda, “Active mitigation of nonlinear noise processes using a novel filtered-s LMS algorithm,” *IEEE Trans. Speech Audio Processing*, vol. 12, pp. 313-322, May 2004.

[5] A. Carini and G. L. Sicuranza, “Transient and steady-state analysis of Filtered-X Affine Projection algorithms,”, *IEEE Trans. Signal Processing*, vol. 54, No. 2, pp. 665- 678, February 2006.